From quasiperiodicity to chaos in the Belousov–Zhabotinskii reaction. I. Experiment

F. Argoul, A. Arneodo, P. Richetti, and J. C. Roux

Citation: The Journal of Chemical Physics **86**, 3325 (1987); doi: 10.1063/1.452751
View online: http://dx.doi.org/10.1063/1.452751
View Table of Contents: http://scitation.aip.org/content/aip/journal/jcp/86/6?ver=pdfcov
Published by the AIP Publishing

From quasiperiodicity to chaos in the Belousov–Zhabotinskii reaction. I. Experiment

F. Argoul, A. Arneodo,[a] P. Richetti, and J. C. Roux
Centre de Recherche Paul Pascal, Université de Bordeaux I, Domaine Universitaire, 33405 Talence Cedex, France

(Received 1 April 1986; accepted 20 October 1986)

We report on the experimental observation of both a primary and a secondary Hopf bifurcation leading to quasiperiodicity in the Belousov–Zhabotinskii reaction. When taking the BZ system away from these local conditions, we witness the occurrence of chaos which comes with the breaking of the underlying torus into a fractal object. We emphasize that most of the alternating periodic–chaotic sequences studied in the literature are reminiscent of such two-frequency dynamics. We argue about the controversial existence of deterministic chaos in such sequences. We anticipate the results of a numerical and theoretical investigation of these sequences which discards definitely any stochastic objection to chemical chaos.

I. INTRODUCTION

Since the late seventies, experimental evidence of low dimensional deterministic chaotic behavior in the Belousov–Zhabotinskii reaction[1,2] has been accumulating.[3–11] Moreover, as suggested by Ruelle[12] in 1973, when forced far from equilibrium such chemical systems are among the best suited to demonstrate universal properties of nonlinear systems.

Indeed the first experimental strange attractor was observed in the BZ reaction in 1980.[13] Soon thereafter, theoretically predicted properties of these strange attractors were actually observed in real experiments:

(i) The complicated dynamics of trajectories in the phase space was shown to obey a deterministic law; one-dimensional (1D) maps[14,15] constructed from the data have yielded smooth curves instead of broad distributions of points as might be expected if the nonperiodicity was the consequence of stochastic forcing.

(ii) These 1D maps were found to be of a generic single humped shape.[16] Experimental evidence in the BZ reaction, moreover, supports the universal predictive properties of such 1D maps with a single extremum when one control parameter is varied[16]: a few period-doubling bifurcations were isolated before the chaotic threshold[17]; beyond this threshold periodic windows were detected with the order of occurrence as predicted for the universal (U) sequence.[18]

(iii) The largest Lyapunov exponent was computed either on the reconstructed 1D map[19] or directly from measurements of the divergence rate of nearby trajectories using appropriate numerical methods.[20] Both of these approaches converge to the same conclusion: the exponent is definitely positive, which attests to the fact that there is sensitive dependence on initial conditions, the hallmark of deterministic chaos.

(iv) Direct evidence for a tangent bifurcation leading to chaos was obtained in Ref. 21. It fits the theoretical characteristics of type-I intermittency as defined by Manneville and Pomeau.[22]

In spite of this whole set of concordant experimental investigations of the BZ reaction, however, some doubts still remain[23–25] regarding the existence of deteministic chaos in well-controlled nonequilibrium chemical reactions. This skepticism originates from two convergent findings:

(i) The very first published papers[4,7–11] about chemical chaos mainly described a sequence of periodic states separated by so-called chaotic states which looked very much like a "stochastic" mixture of the adjoining periodic states. In spite of "heroic efforts to minimize unavoidable fluctuations"[25] in the control parameter [usually the flow rate in the continuously stirred tank reactor (CSTR)], there has been no direct experimental proof that these nonperiodic states could result from the complexities of the BZ kinetics rather than from fluctuations or some experimental artifacts.

(ii) The well established chemical model of the BZ reaction, the Fields–Koros–Noyes (FKN)[26,27] model or its reduced versions (oregonators)[28–32] were shown to display very similar sequences. Numerical simulations of such models, however, yielded time series which always looked periodic.[23,30–32] Attempts to figure out what happened in between two consecutive periodic states by scanning the control parameter very accurately, have revealed new very complicated states,[23,30–32] but apparently still no chaos.

At this point let us emphasize that in these last experiments as well as in the simulations, the distinction between periodic and chaotic states was only based on a visual inspection of the time series (sometimes together with an examination of the power spectra). The periodic–chaotic sequences under discussion in both these experimental and numerical studies of the BZ reaction, moreover, occur in a parameter domain very different from the set of constraints investigated in the Texas experiment,[15,17–19] where the inescapable evidence of deterministic chaos described earlier was obtained.

The main challenge of our study of the BZ reaction will be to address both of these objections. Here, using the main tools inspired from dynamical systems theory,[33,34] i.e., the reconstruction from a single time series of multidimensional phase portraits[35,36] as well as Poincaré maps and first return maps, we propose a new understanding of the so-called alternating periodic–chaotic sequences in terms of dynamics involving two fundamental frequencies. The first step of our

[a] Permanent address: Laboratoire de Physique Théorique, Université de Nice, Parc Valrose, 06034 Nice Cedex, France.

 0021-9606/87/063325-14$02.10

TABLE I. Summary of observations of complex dynamics in the BZ reaction. The chemical concentrations are given relative to the reference concentrations in Ref. 7: malonic acid = 0.3 mol/ℓ; sodium (or potasium) bromate = 0.14 mol/ℓ; cerous sulfate = 0.001 mol/ℓ; sulfuric acid = 0.2 mol/ℓ.

Experiment	Malonic acid	Sodium bromate	Cerous sulfate	Sulfuric acid	Residence time (h)	Temperature	Stirring rate (rpm)	Dynamics
Virginia (Refs. 3, 7, and 14)	1	1	1	1	0.08 0.15	25	2000	Periodic-chaotic sequence (first evidence)
Texas (Refs. 15, 17, and 19)	0.83	1	0.83	1	0.5 3.0	28.3	1500	Periodic-chaotic sequence (1 frequency)
Texas (Refs. 61 and 62)	0.27	0.2	Mn^{++} 0.42	8.5	0.08 0.14	25	1800	Periodic-chaotic sequence (2 frequencies)
Bordeaux (Refs. 8, 11, 13, 58, and 59)	0.26	0.26	0.25	7.2	0.03 0.21	39	600	Periodic-chaotic sequence (2 frequencies)
Bordeaux (Ref. 21)	0.19	0.013	0.58	7.5	0.02 2.0	39.6	600	Type-I intermittency
Experiment 1 (Ref. 50)	0.22	0.016	0.17	3.15	0.25 1.0	43	600	Primary Hopf bifurcation
Experiment 2 (Ref. 52)	0.58	0.086	0.083	5	0.33 0.6	43	600	Secondary Hopf bifurcation
Experiment 3 (Refs. 56 and 57)	0.55	0.086	0.083	5	0.05 0.1	40	600	Fractal torus
Experiment 4 (Ref. 77)	0.17	0.18	0.17	5	0.41	43	600	Periodic-chaotic sequence (2 frequencies)
Experiment 5 (Ref. 77)	0.11	0.03	0.17	7.5	0.2 0.55	43	600	Periodic-chaotic sequence (2 frequencies)

experimental investigation of the BZ system is thus to report on the actual occurrence of quasiperiodic behavior in this reaction. This paper is organized as follows:

In Sec. II, we provide experimental evidence of a transition from the thermodynamic branch to nearly sinusoidal small amplitude oscillations, which fits remarkably the Landau–Hopf formalism.[33,34,37,38] In nearby but very well located conditions in parameter space, we point out that the BZ system can display a secondary Hopf bifurcation leading to quasiperiodicity.[39] In Sec. III, we discuss the transition from quasiperiodicity to chaos when taking the BZ system away from this local situation. The breaking of the underlying torus into a fractal object is clearly exhibited. In Sec. IV we investigate the alternating periodic–chaotic sequences as reminiscent of two-frequency dynamics. We convince ourselves that such sequences are less suited to study nonperiodicity in the BZ reaction than the "period-adding" sequence well characterized in the Texas experiment.[15,17–19] We emphasize that such an experimental analysis requires a complementary numerical study of a chemical model together with the assistance of dynamical system theory in order to clear up the controversy and to conclude definitively that deterministic chaos exists. Both the modeling and theoretical analysis will be the subject of a second paper II,[40] as referenced in the remaining of the present paper. Section V is devoted to concluding remarks. Table I lists the experimental conditions used in our different studies of the BZ reaction as compared to previous experiments.

II. QUASIPERIODICITY

In the past decade the BZ reaction has become the prototype for experimental and theoretical studies of the rich variety of nonlinear dynamical behaviors displayed by chemical systems when they are forced far from equilibrium.[41–43] Early on, the question was about the status of the chaotic behavior observed in the experiments and a lot of effort was devoted to the identification of well-known scenarios to weak turbulence.[44,45] However, no detailed quantitative experimental investigation of the onset of oscillatory dynamics in the BZ reaction had ever be done.

In this section we first report measurements both below and above the onset of time-dependent dynamics in the BZ reaction when starting on the thermodynamic branch and

increasing the total inlet flow of the reactants through the reactor. Then with only few changes in the external constraints, we witness a secondary Hopf bifurcation leading to a quasiperiodic regime. As compared to the classic (supercritical) primary Hopf bifurcation, this secondary bifurcation presents some degrees of degeneracy[34,38,39]; this feature together with the further evolution of the underlying T^2 torus are very characteristic of the interaction of the two generic instabilities in the BZ reaction[46,47]: the (previous) Hopf bifurcation at the origin of the oscillating nature of this reaction and the hysteresis (stationary) bifurcation which accounts for the phenomenon of bistability.[48,49] In this section, we will remain at a descriptive level; we refer the reader to paper II for a tentative theoretical interpretation.

A. Birth of nearly sinusoidal oscillations: Primary Hopf bifurcation (Ref. 50)

The BZ reaction is conducted in a CSTR fed by three feed lines (Fig. 1). The chemicals used are of the best commercial grade available (PROLABO Rectapur) (unit N = 0.5 mol/ℓ = 0.5M):

Experiment 1:

F1: $[NaBrO_3] = 6.5\times10^{-3}$ M, $[H_2SO_4] = 0.8$ N,
F2: $[CH_2(COOH)_2] = 0.20$ M, $[H_2SO_4] = 1.5$ N,
F3: $[Ce_2(SO_4)_3] = 5\times10^{-4}$ M, $[H_2SO_4] = 1.5$ N.

The three fluxes are maintained nearly equal, using a peristaltic pump, while the overall flow through the reactor (λ) plays the role of the bifurcation parameter; the investigation flow domain is [0.1 ml/min, 0.7 ml/min]. The dynamics is monitored by the absorbance of the solution at 360 nm; the stirring rate is 600 rpm; while the temperature is regulated to 43 °C. With this choice of the experimental constraints, the thermodynamic branch is asymptotically stable

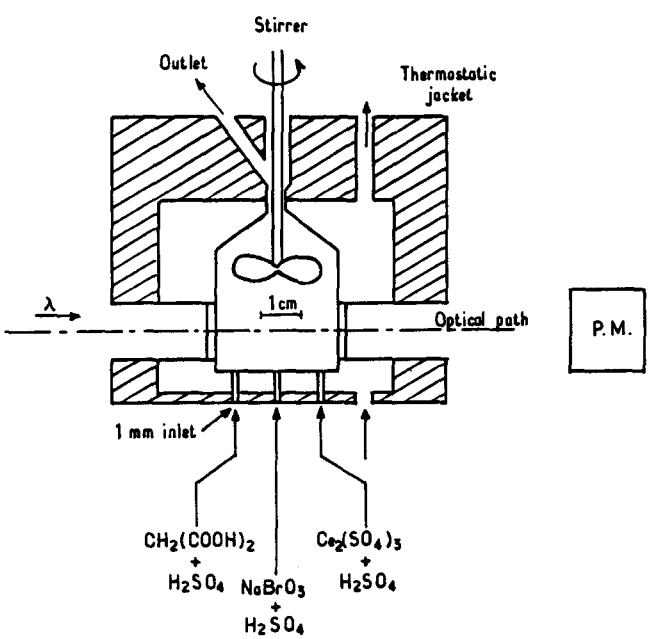

FIG. 1. Scale scheme of the thermostated reactor.

at low flow rate up to some critical value λ_c which denotes the transition to a time dependent regime. Below λ_c, the relaxation time τ of the oscillatory envelop of the transients diverges when approaching λ_c according to the equation

$$\tau \sim |\lambda - \lambda_c|^{-\alpha}; \tag{1}$$

τ vs $|\lambda - \lambda_c|/\lambda_c$ is plotted on a log–log scale in Fig. 2(a); a least-squares fit to the data yields $\alpha = 0.98 \pm 0.05$. Above λ_c, the amplitude of the nearly sinusoidal periodic oscillations increases continuously from zero with a dependence in $\lambda - \lambda_c$ which is well fitted with the equation:

$$A \sim (\lambda - \lambda_c)^{\beta}, \tag{2}$$

as shown on a log–log scale in Fig. 2(b); β is found to be $\beta = 0.51 \pm 0.02$ while $\lambda_c = 0.16 \pm 0.005$ ml/min. [In order to avoid duplications of results, we refer the reader to Fig. 3(a) for the illustration of both the time series and power spectrum and to Fig. 4(a) for the reconstructed phase portrait of a typical nearly sinusoidal periodic signal.] Both these experimental estimates of the exponents α and β are in remarkable agreement with the classical theoretical predictions for a generic supercritical Hopf bifurcation[33,34,37,38], namely

$$\alpha = 1 \text{ and } \beta = 1/2. \tag{3}$$

This first test of the Landau–Hopf formalism in the BZ reaction deserves a few comments. There have been some experimental investigations of the onset of oscillatory behavior in this reaction; some of them have succeeded in detecting a subcritical Hopf bifurcation,[51] but they all have failed to identify a supercritical bifurcation as predicted from numerical simulations of more or less realistical models.[49] Our experiment points out that such a supercritical Hopf bifurcation does exist in an accessible range of parameters values. We have deliberately emphasized the classical properties of this primary Hopf bifurcation in order to be able later on to distinguish between a nondegenerate Hopf bifurcation which satisfies the power laws (1), (2), and (3) and a degenerate Hopf bifurcation which differs in the measure of β ($\beta < 1/4$). Such a discrimination will be one of the main result of the following subsection; indeed, the experimental evidence of a degenerate secondary Hopf bifurcation will be one of the fundamental observations which will allow us in paper II to go further towards understanding the nature and origin of the resulting quasiperiodic regime.

B. Transition from periodic to quasiperiodic oscillations: Secondary Hopf bifurcation (Ref. 52)

This second experiment is conducted under the following set of constraints:

Experiment 2:

F1: $[NaBrO_3] = 3.6\times10^{-2}$ M, $[H_2SO_4] = 1.5$ N,
F2: $[CH_2(COOH)_2] = 0.525$ M, $[H_2SO_4] = 3$ N,
F3: $[Ce_2(SO_4)_3] = 2.5\times10^{-4}$ M, $[H_2SO_4] = 1.5$ N.

The overall investigated flow domain was [0.3 ml/min, 0.5 ml/min], a rather tiny control parameter range. The observed time series and power spectra are shown in Fig. 3,

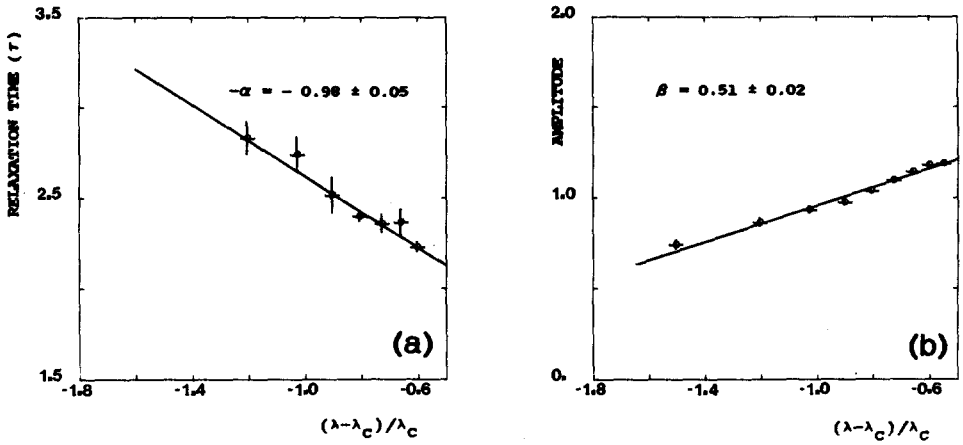

FIG. 2. (a) Characteristic relaxation time τ of the oscillatory envelop vs $|\lambda-\lambda_c|/\lambda_c$ plotted on a full logarithmic scale; the circles correspond to a perturbation of the steady state through a bromide injection at fixed values of the flow rate ($\lambda<\lambda_c$); the solid line is a least-squares fit which yields $\alpha=0.98\pm0.05$. (b) Amplitude of the periodic oscillation ($\lambda>\lambda_c$) vs $(\lambda-\lambda_c)/\lambda_c$ plotted on a full logarithmic scale; the solid line is a least-squares fit which yields $\beta=0.51\pm0.02$.

while Fig. 4 illustrates the corresponding phase portraits which are constructed using the time delay method. All these results are obtained from digitized data with a sampling time of 150 ms. In both these figures, four situations are selected which allow a tight description of the entire scenario: (a) the original periodic regime; (b) the transition to quasiperiodicity; (c) the evolution of the torus; (d) the death of the torus. The respective Poincaré cross sections obtained by looking at the successive intersections of the trajectories with an arbitrary transverse plane are represented in Fig. 5. These experimental Poincaré maps together with the phase portraits give a better insight into the evolution of the shape of the torus.

1. The original periodic regime: $\lambda=0.34$ ml/min

As illustrated in Figs. 3(a) and 4(a), the original periodic regime is nearly sinusoidal with only a few harmonics of the fundamental frequency f_1 ($\sim$40 mHz) above the noise level. These small amplitude oscillations are very likely to result from a primary Hopf bifurcation as the one discussed in Sec. II A.

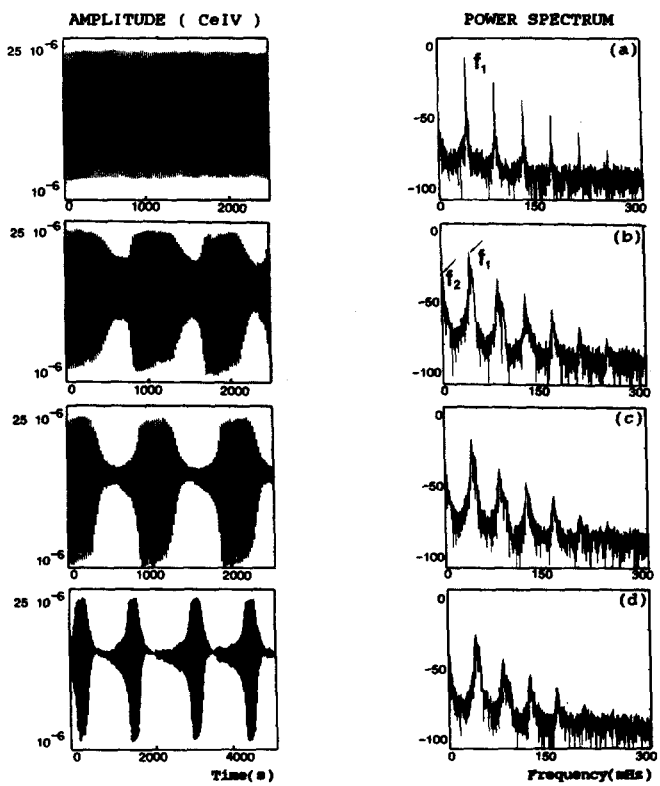

FIG. 3. Time series and power spectra (in db) for the four steps of the scenario observed in the BZ reaction with the set of constraints defined in Experiment 2. (a) $\lambda=0.34$ ml/min: the original periodic regime; (b) $\lambda=0.355$ ml/min: the transition to a quasiperiodic regime; (c) $\lambda=0.36$ ml/min: the evolution of the torus; (d) $\lambda=0.43$ ml/min: the torus near its death; the experimental uncertainty in measuring the flow rate is estimated to be about 5×10^{-3} ml/min. Note the change in time scale from the time series (a), (b), (c) to the time series (d).

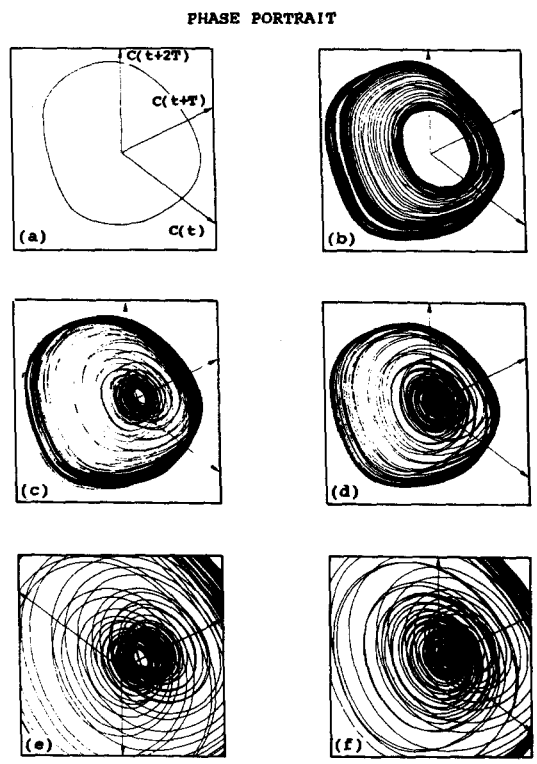

FIG. 4. Phase portraits corresponding to the time series of Fig. 3 (a), (b), (c), and (d); (e) and (f) are enlargements of the inner part of the torus presented in (c) and (d), respectively. The trajectories are constructed in a three-dimensional phase space using the time delay method with a time delay $T=4.5$ s.

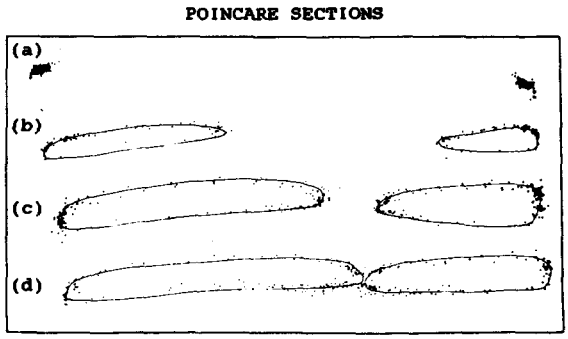

FIG. 5. Intersections of the 3D phase space trajectories of Figs. 4(a)–4(d) with an arbitrary transversal plane.

2. The transition to a quasiperiodic regime: $\lambda = 0.355$ ml/min

With a very small increase in the flow rate, the system switches from a periodic to a quasiperiodic regime

(i) On the time series of Fig. 3(b) one can notice the appearance of a slow periodic modulation of the amplitude of the original nearly sinusoidal oscillations. The amplitude of this modulation is immediately obvious although the difference $\Delta\lambda = 0.015$ ml/min from situation (1) to situation (2) is small and comparable to the unavoidable fluctuations in the flow rate. Indeed the stiffness of this transition comes with experimental difficulties in stabilizing intermediate states such as (2) for more than a few hours.

(ii) On the power spectrum of Fig. 3(b), the new frequency f_2 is much smaller than f_1, i.e., $f_2/f_1 \sim 1/30$. The apparent widening of the fundamental peak and its harmonics results from the abundance of secondary harmonics $f = nf_1 + mf_2$.

(iii) The corresponding phase portrait in Fig. 4(b) displays a toroidal attractor. Intersections by planes nearly perpendicular to most of the trajectories clearly delimit closed curves with smooth elliptic shapes as seen in Fig. 5(b). This is a strong indication that the dynamics lies on a torus. Moreover, although the characteristic recording duration of a typical experiment at a given flow rate is finite and of the order of a few hours, it is enough to convince oneself that the trajectories fill up this toroidal surface ergodically.

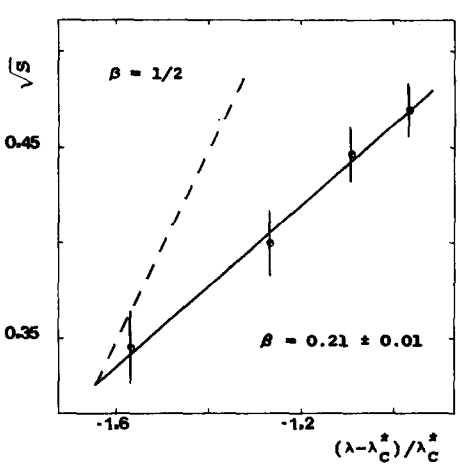

FIG. 6. The square root $\sqrt{S}$ of the area of the elliptic Poincaré sections in Fig. 5 vs $(\lambda - \lambda_c^*)/\lambda_c^*$ plotted on a full logarithmic scale; $\lambda_c^* = 0.350 \pm 0.005$ ml/min is the measured transition value to quasiperiodicity. The solid line is a least-squares fit which yields $\beta = 0.21 \pm 0.01$. Such an estimate of the exponent β rules out the classical value $\beta = 1/2$ (dashed line) and strongly suggests that the secondary Hopf bifurcation is degenerate.

3. The evolution of the torus: $\lambda \in$ [0.36 ml/min, 0.43 ml/min]

When increasing the flow rate further, the amplitude of the modulation keeps growing as shown on the time series of Fig. 3(c). Such an evolution manifests itself on the phase portrait of Fig. 4(c) and the Poincaré section of Fig. 5(c) as an increase of the global size of the torus at the expense of the size of its inner part which shrinks to a thin tube. On the power spectra, this scenario is associated with a decrease of the low frequency f_2 (and thus the appearance of more harmonics) which means that the thinner the center hole, the larger the duration of time spent by the trajectory inside the hole.

4. The death of the torus: $\lambda > 0.45$ ml/min

When one reaches values of $\lambda \geqslant 0.45$ ml/min, the time series displays larger and larger windows of nearly stationary behavior interrupted from time to time by bursts of large amplitude oscillations [Fig. 3(d)]. With a further increase in the flow rate, the system ultimately changes to a steady state (the flux branch) which belongs to its inner part [Figs. 4(d) and 5(d)]. As seen on the power spectra, the death of the torus is associated with the general trend of the ratio f_2/f_1 decreasing to zero.

Beyond this rather qualitative description of the entire scenario, one may wonder whether or not the bifurcation which leads to the quasiperiodic state fits the classical Landau–Hopf formalism[33,34,37–39] for supercritical bifurcation. To draw a bifurcation diagram we need to consider a variable which reflects the toroidal geometry of the attractor. In Fig. 6, the square root of the area of the ellipses which constitute the Poincaré sections in Fig. 5, is plotted as a function of the flow rate $[(\lambda - \lambda_c^*)/\lambda_c^*]$ on a log–log scale. The stiffness of the transition is clearly shown on such a diagram. The classical square root law (2) with $\beta = 1/2$ is rather unlikely to fit our data; a value $\beta \leqslant 1/4$ seems to be more appropriate. However a more accurate estimate of the exponent β would require more measurements in the intermediate λ range [0.35 ml/min, 0.36 ml/min]. This raises up severe technical problems since the unavoidable fluctuations in the flow rate are of the same order of magnitude as the parameter range we want to explore. Within our experimental resolution, we do not detect any hysteresis effect at the transition to quasiperiodicity. This, together with our estimate of β, strongly suggests that the secondary Hopf bifurcation is degenerate.

By looking at the successive Poincaré sections in Fig. 5, we do not see any distortion of the torus at any stage of its evolution. There is no evidence of stretching or folding effects which could lead to a fractal object.[53–55] The accumulation of experimental points at the inner part of the torus just

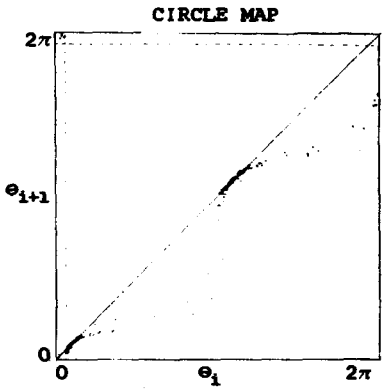

FIG. 7. The circle map $\theta_{i+1}=f(\theta_i)$ is constructed from the Poincaré section in Fig. 5(d), the angle θ is defined with respect to an arbitrarily chosen axis which originates inside the ellipsis.

preannounces the appearance of a stable steady state. In order to have a better insight onto the dynamics we have plotted in Fig. 7 a map of the circle onto itself: $\theta_{i+1}=f(\theta_i)$ mod 2π, as obtained from the Poincaré section of Fig. 5(d). The angle θ is defined with respect to an arbitrarily chosen axis which originates at a given point located inside the ellipses. Such a map is invertible (to the precision of the data) and referring to the theory of diffeomorphisms of the circle[33,34,39] we can assert that no chaos is to be expected in this experiment [the circle maps corresponding to regimes (2) and (3) present the same property of invertibility]. The power spectra of Fig. 3 with no clear evidence of broadband noise seem to corroborate such a conclusion. No frequency lockings between f_1 and f_2 were detected during our experiment. The actual occurrence of quasiperiodicity will be discussed in paper II.

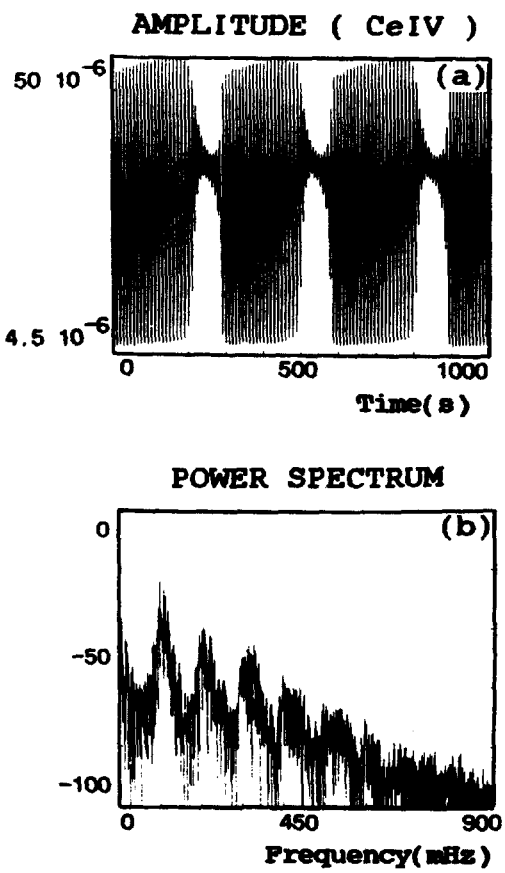

FIG. 8. Time series (a) and power spectrum (b) of a chaotic regime involving two characteristic frequencies: $f_1\sim 103$ mHz and $f_2\sim 2.5$ mHz; the experiment was conducted with the set of constraints defined in Experiment 3.

III. CHAOS ON A FRACTAL TORUS (REF. 56)

In the previous section, we have emphasized that the existence, the shape as well as the entire evolution of the torus observed in Experiment 2 and illustrated in Figs. 3–7, are very characteristic of a rather small domain in parameter space. A slight displacement from these specific conditions induces modifications of the overall features of this torus. In this section, we report the results of a third experiment on the BZ system which corresponds to the following chemical feeding fluxes:

Experiment 3:

F1: $[NaBrO_3]=3.6\times10^{-2}$ M, $[H_2SO_4]=1.5$ N,
F2: $[CH_2(COOH)_2]=0.5$ M, $[H_2SO_4]=3.0$ N,
F3: $[Ce_2(SO_4)_3]=2.5\times10^{-4}$ M, $[H_2SO_4]=1.5$ N.

One must mention that this experiment on the BZ system had been performed with a different experimental device (free surface CSTR); henceforth the reader is aware that a comparative study of both these experiments has to remain at a qualitative level only.

When increasing the control parameter from low flow rate values, we observe the same sequence of events as related in Fig. 3. The time series and power spectrum of a typical intermediate state are shown in Fig. 8. At first sight, there is a quantitative change in the size of the oscillations as well as in the value of the fundamental frequency f_1. The concentration of Ce^{4+} now oscillates in between 4.5×10^{-6} and 50×10^{-6} M (instead of 10^{-6} and 25×10^{-6} M in Fig. 3) with a fundamental frequency $f_1\sim103$ mHz (instead of $f_1\sim35$ mHz in Fig. 3). The main trends of the sequence, however, are apparently preserved such as the smallness of the ratio of the modulation frequency to the fundamental frequency which is measured to be about $f_2/f_1\sim1/40$. If one focuses on the time series of Fig. 8(a), it looks very like a quasiperiodic signal. Nevertheless, from a careful examination of the signal-to-noise ratio in the power spectrum in Fig. 8(b), one suspects an anomalous strengthening (with respect to the corresponding power specta in Fig. 3) of the noise level which might be an indication for the existence of chaos.

The reconstruction of the corresponding attractor is shown in Figs. 9(a) and 9(b). We notice with these phase portraits that together with an overall swelling of the torus, there is a deformation of its shape. The Poincaré sections 1,3 and 2,4 presented in Figs. 9(c) and 9(d) and corresponding to the intersection of the torus by two planes which contain its axis, bring a new insight into the real fractal nature of this torus. If one concentrates on the points which belong to the rectangle drawn in Fig. 9(d) (where the points corresponding to the visit of the center hole of the torus are excluded for convenience), one can guess a stretching (between sections 1 and 2) and a folding (sections 2, 3, and 4) which are a necessary consequence of the exponentially fast separation of

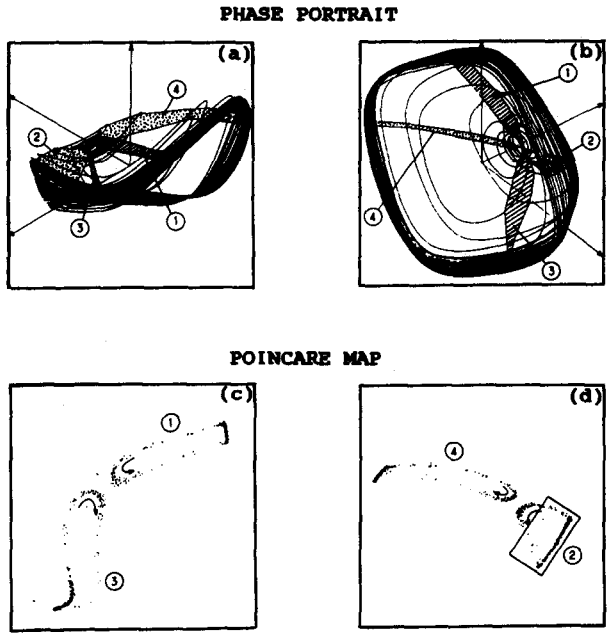

FIG. 9. Phase portraits and Poincaré maps corresponding to the time series of Fig. 8(a). Two views of the attractor are shown in (a) and (b) using the time delay method with a time delay $T = 2$ s. (c) and (d) represent the Poincaré maps associated with the two planes shown in (a); (d) is reduced by a factor 5/6 with respect to (c).

nearby trajectories in any strange attractor. Such stretching and folding effects become clearer on the Poincaré map shown in Fig. 10,[57] where the intersecting plane is defined nearly tangent to the trajectories in the outer part of the torus; such a plane does not cross the trajectory when it goes through the center hole of the torus. The missing points which correspond approximately to the points which lie out of the rectangle in Fig. 9(d) would be located in the dashed area which has been drawn to guide the eye.

Such a fractal structure of the torus is associated with some mixing of the trajectories which can be traced in any Poincaré section as a disruption of the monotoneous ergodic covering of the torus; the consecutive intersections display a back and forth movement in the part of the map where the folding occurs. This erratic dynamics is made clear on the circle map shown in Fig. 11; the mixing process manifests itself simply as a thickening of the curve which is no longer single valued (compared to Fig. 7)[53–55] in the region labeled M which corresponds to a range of θ values characteristic of the points which lie in the rectangle in Fig. 9(d). There is a second region where points accumulate, labeled SN, which corresponds to points lying on the torus axis. This slowing down of the dynamics near the torus axis preannounces the occurrence of a stable steady state which will emerge via a saddle-node bifurcation. Within our experimental resolution, this bifurcation coincides with the death of the fractal torus since when reversing the variation of the flow rate we have not detected any hysteresis phenomenon and thus no bistability between the fractal torus and the final steady state which survives at high flow rate (the flux branch).

IV. THE PERIODIC-CHAOTIC SEQUENCES

If one goes on moving the BZ system away from the local quasiperiodic situation described in Sec. II, the fractal torus depicted in Sec. III evolves dramatically. Figure 12 illustrates a chaotic state observed in a fourth experiment for the following set of chemical concentrations:

Experiment 4:

F1: $[NaBrO_3] = 7.5\times10^{-2}$ M, $[H_2SO_4] = 2$ N,
F2: $[CH_2(COOH)_2] = 0.15$ M, $[H_2SO_4] = 2$ N,
F3: $[Ce_2(SO_4)_3] = 5\times10^{-4}$ M, $[H_2SO_4] = 2$ N.

The investigated value of the flow rate is $\lambda = 0.4$ ml/min. The toroidal aspect of the oscillations is less striking than in the previous experiments. Two different regimes can be distinguished on both the time series and the phase portraits in Figs. 12(a) and 12(c), respectively: large amplitude oscillations which get more and more like relaxation type and small amplitude oscillations which are reminiscent of the oscillations in the inner part of the torus in Experiments 2 and 3. As seen on the phase portrait, the trajectories have become more concentrated in one band around the torus, the size of which has considerably increased since the amplitude of the relaxation oscillations is four times larger than the amplitude of the quasiperiodic oscillations in Experiment 2. We can also notice that the trajectories seem to converge when entering the center hole and to diverge when leaving it; this produces a wide distribution in the amplitude of the last small oscillation which in turn induces a variation in the number of the following large amplitude oscillation (we have observed from seven up to nine large amplitude oscillations). This suggests that the trajectory displays an extreme

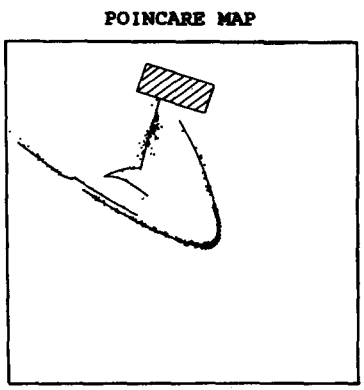

FIG. 10. A Poincaré section which misses the center hole of the torus (sketched by the shaded area) but enlightens the stretching and folding properties of the dynamics.

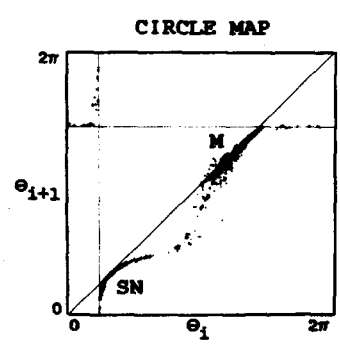

FIG. 11. A circle map built from section 1 of Fig. 9 (c). Both the accumulations of points labeled M and SN, respectively, are discussed in the main text.

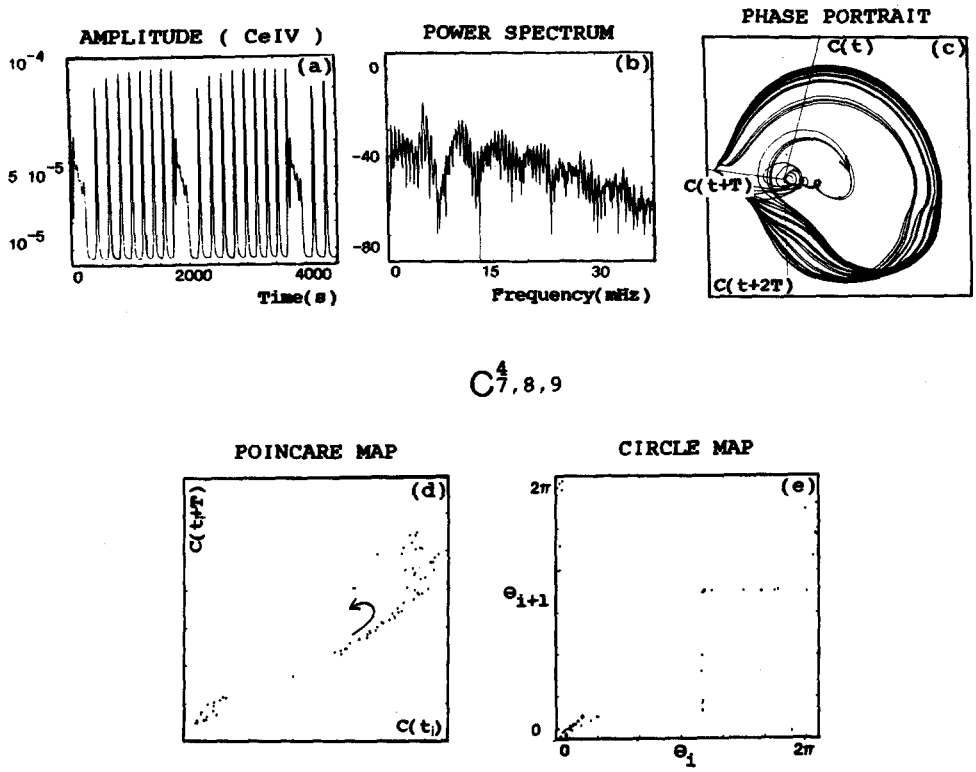

FIG. 12. A chaotic state $C^4_{7,8,9}$ observed in the BZ system for the set of chemical concentrations defined in Experiment 4 and a flow rate $\lambda = 0.4$ ml/min. (a) The time series; (b) the power spectrum; (c) a phase portrait (the time delay $T = 2.5$ s); (d) a Poincaré map; (e) a circle map.

sensitivity when visiting the center hole of the torus and approaches the unstable (saddle) focus which belongs to its axis (see paper II).

Since there is no longer a fundamental frequency f_1 and a superimposed modulation frequency f_2, but two drastically different characteristic times $t_L \sim 190$ s and $t_s \sim 65$ s corresponding, respectively, to the "pseudoperiod" of the large and small amplitude oscillations [Fig. 12(b)], an estimate of the winding number requires the definition of a Poincaré map and its corresponding circle map.[33,34,39] These maps are shown in Figs. 12(d) and 12(e), respectively; in spite of the poor statistic of this experiment, one can see that the whole set of points of the Poincaré map lies roughly on a closed curve (the duration of this experiment is around 4 h, which allows a record of about 80 intersections of the trajectory with the Poincaré plane; but many more points are needed if one intends, as in Sec. III, to study the fractal nature of the torus). Then, defining an angular coordinate θ with respect to an arbitrary axis originating inside this closed curve, one can analyze the dynamics of this phase, through the iteration of the circle map $\theta_{i+1} = f(\theta_i)$ where θ_i is the value of θ at the ith intersection of the trajectory with the Poincaré plane [Fig 12(e)]. In particular one can compute the winding number

$$W = \lim_{n\to\infty} [(f^n(\theta) - \theta)/2n\pi] \tag{4}$$

which comes out equal to $W \sim 1/12$ (for an operational estimation of W, we refer the reader to paper II), a value which is considerably larger than the ratio $W = f_2/f_1 \sim 1/30$ characteristic of the quasiperiodic regime observed in Experiment 2, and the estimate $W \sim 1/40$ when wandering over the fractal torus described in Experiment 3.

A. Description of the periodic-chaotic sequences

In this fifth experiment, we reinvestigate a one-parameter path in the parameter space,[58,59] which consists in increasing the flow rate from $\lambda \sim 0.3$ up to 0.75 ml/min for a set of reactant concentrations which differs from Experiment 4 mainly in the concentration of the sulfuric acid and sodium bromate.

Experiment 5:

F1: $[NaBrO_3] = 10^{-2}$ M, $[H_2SO_4] = 3$ N,
F2: $[CH_2(COOH)_2] = 0.1$ M, $[H_2SO_4] = 3$ N,
F3: $[Ce_2(SO_4)_3] = 5\times10^{-4}$ M, $[H_2SO_4] = 3$ N.

At a low flow rate ($\lambda \sim 0.3$ ml/min), the system exhibits periodic oscillations which are strongly relaxing as shown in Fig. 13(a) both on the time series and in the power spectrum where many harmonics of the fundamental frequency emerge from the noise level. When increasing the flow rate through the first critical value, small amplitude oscillations appear, disrupting more or less regularly the large amplitude relaxation oscillations and introducing a second characteristic time into the dynamics. When increasing the flow rate, we observe a succession of periodic and nonperiodic states. Time series records, power spectra, and reconstructed phase portraits of some of the states of this sequence are shown in Fig. 13. Within the experimental resolution, the following ordering has been recorded:

$$P^0_1, C^1_{n_1,\ldots,n_i}(n_i \geqslant 4), C^1_{3,4}, P^1_3, C^{1,2}_3, P^2_3, P^3_3, \ldots, C^{4,5}_3,$$
$$P^1_2, P^{1,2}_2, P^2_2, P^3_2, \ldots, C^n_2(n \sim 10), C^n_{1,2}, C^n_1; \tag{5}$$

where P and C stand for periodic and chaotic states, respectively; the upper index defines the number of small amplitude oscillations in a basic pattern, while the lower index

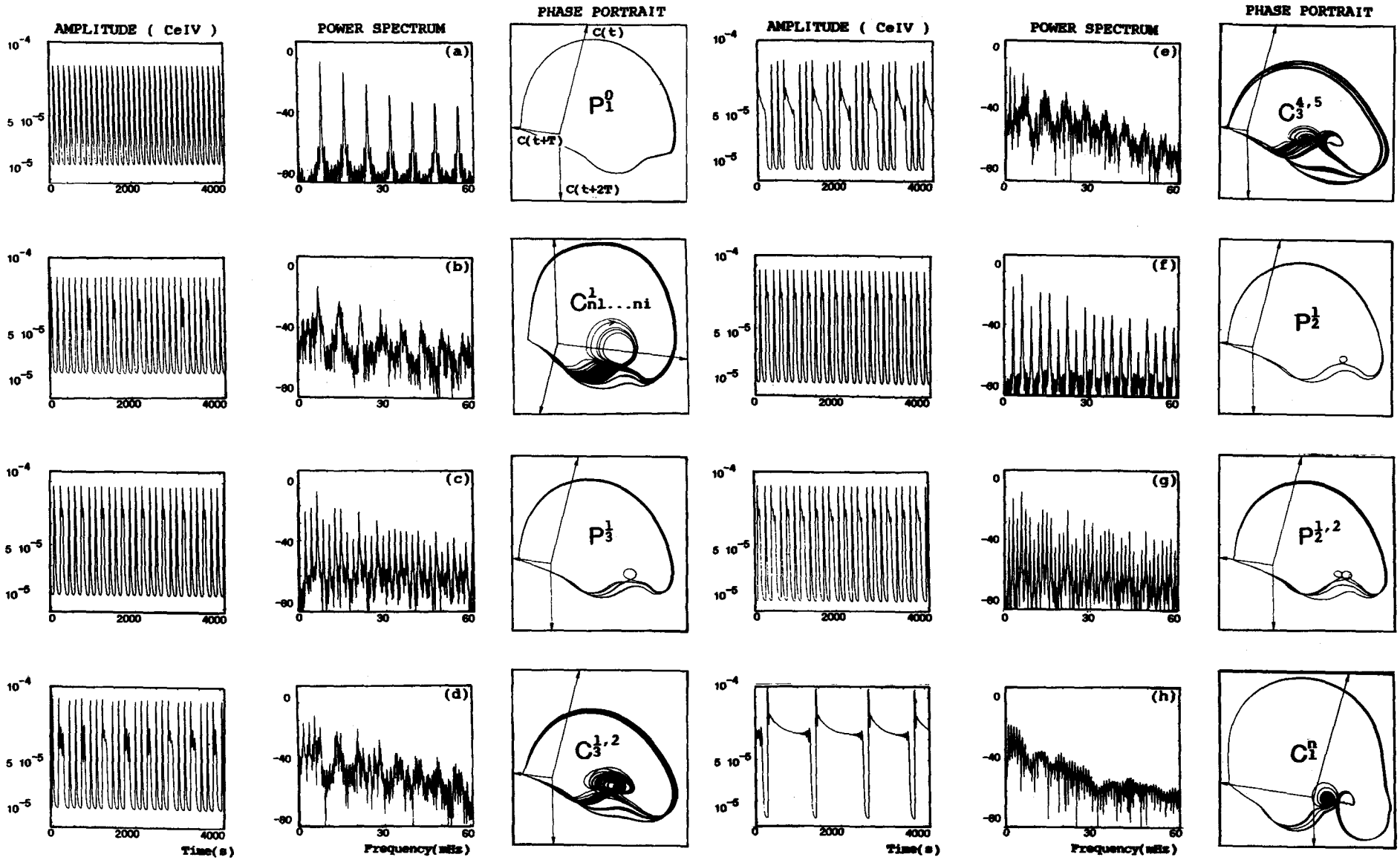

FIG. 13. Selected steps of the periodic–chaotic sequence observed in the BZ reaction with the set of constraints defined in Experiment 5; the time series, the power spectrum, and the reconstructed phase portrait are represented [the time delay $T = 2.5$ s except for (b) and (h) where $T = 3.5$ s]: (a) $\lambda = 0.30$ ml/min: P_1^0; (b) $\lambda = 0.35$ ml/min: $C^1_{n_1,\ldots,n_i}$; (c) $\lambda = 0.40$ ml/min: $P_3^{\frac{1}{3}}$; (d) $\lambda = 0.45$ ml/min: $C_3^{\frac{1}{3},2}$; (e) $\lambda = 0.55$ ml/min: $c_3^{4,5}$; (f) $\lambda = 0.555$ ml/min: $P_2^{\frac{1}{2}}$; (g) $\lambda = 0.57$ ml/min: $P_2^{\frac{1}{2},2}$; (h) $\lambda = 0.72$ ml/min: C_1^n. The experimental resolution in the flow rate is about 5×10^{-3} ml/min.

denotes the number of large amplitude relaxation oscillations (e.g., P_2^3 means a periodic state with two large and three small oscillations).[60] Beyond a second critical value of the flow rate, there is no more oscillating state and the system ends in a stationary state (the flux branch).

Similar sequences have been already observed in several experiments[4,7,58,59] as well as in numerical simulations of modified Oregonators.[23,30–32] As mentioned in the Introduction, all the arguments about the status of the chaotic behavior in the BZ reaction have been focused on such sequences. Does such chaos result from nonlinear complexities of the BZ kinetics or from some experimental artifacts? The chaotic states $C_i^{j,j+1}$ look very much like a "stochastic" mixture of P_i^j and P_i^{j+1} patterns: are they deterministic regimes or simply the consequence of some random fluctuations in the control parameter, driving stochastically the system back and forth from P_i^j to P_i^{j+1}? Such a skepticism is strengthened by very recent experimental results by Maselko and Swinney[61,62] who have observed in the BZ reaction a complex sequence of periodic states which look very like the ones involved in the sequence shown in Fig. 13. Suspecting that the underlying dynamics involves two frequencies, these authors have defined a winding number in a rather phenomenological way and have shown that it is a function of the control parameter very similar to a complete devil's staircase; the ordering of the periodic states is such that the winding number satisfies the Farey relationship,[63] i.e., between states with $W = a/b$ and c/d lies a state with $W = (a+b)/(c+d)$. This result comes with the fact that neither quasiperiodic nor chaotic states are observed in this experiment.

Our goal in this section is to complete the previous analysis of these complex sequences which were based essentially on the examination of the time series and corresponding power spectra. Through the reconstruction of phase portraits, Poincaré maps, and circle maps we bring new insight into these alternating periodic–chaotic sequences: they are reminiscent of a dynamics with two fundamental frequencies[7] as discovered in Secs. II and III. This will lead us to classify these sequences into two distinct families:

(i) The sequences which involve only one fundamental frequency and which, like those observed in the Texas experiment, exhibit "macroscopic" deterministic chaos easily detectable experimentally.[15,17–19]

(ii) The sequences like the one shown in Fig. 13 (and which were the most studied) involving two fundamental frequencies and which display "microscopic" (in the sense that it is located in a tiny region of the phase space) chaos hardly accessible from an experimental point of view.[4,7,8,11,13,58,59]

This distinction enlightens the controversy which has matched the "pro" deterministic against the prostochastic chemists (they were not speaking about the same sequence of events) for years and years. A real understanding of these last sequences is only possible through a confrontation of experiments with simulations. With the assistance of the theory of dynamical systems we will be able in paper II to conclude definitely to the existence of deterministic chaos.

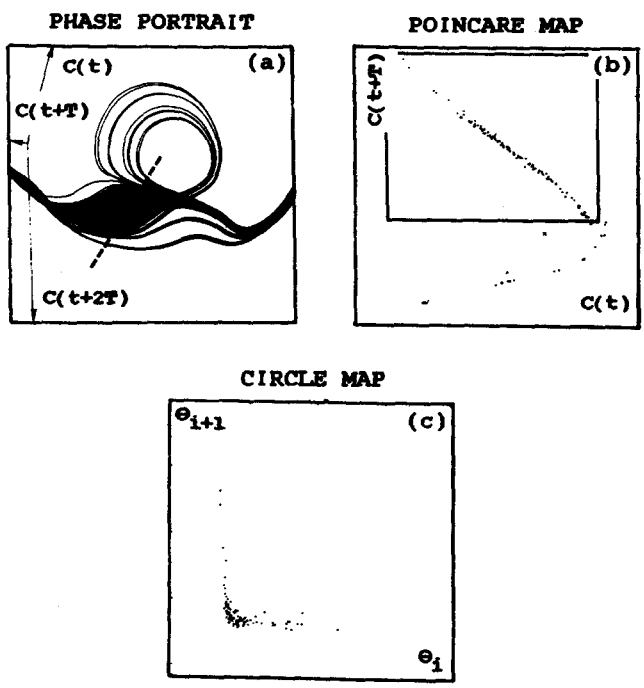

FIG. 14. Description of the first step of the periodic–chaotic sequence reported in Fig. 13; $\lambda = 0.35$ ml/min: $C^1_{n_1,\ldots,n_i}$. (a) An enlargement of the phase portrait shown in Fig. 13(b); (b) a Poincaré map [the Poincaré plane is materialized by the dashed line sketched in (a)]; (c) a circle map limited to the points which lie in the rectangle drawn in (b).

1. The transition to chaos: $\lambda = 0.35$ ml/min

The transition between the relaxation oscillations P_1^0 and the nonperiodic regime $C^1_{n_1,\ldots,n_i}$ is shown in Figs. 13(a) and 13(b). When λ crosses the critical value $\lambda_t \sim 0.35$ ml/min, a small amplitude oscillation once in a while disrupts erratically the large amplitude relaxation oscillations. At first sight such a transition is reminiscent of intermittency[22]: there are long intervals of nearly periodic behavior (the relaxation oscillations) between occasional bursts of chaos (the small amplitude oscillations). As seen in Fig. 13(b), the power spectrum displays a characteristic broadband noise with sharp peaks reminiscent of the periodic regime. The chaotic aspect of the small amplitude oscillations is fascinating in the phase portrait: the sensitive dependence on initial conditions[64] is striking and results from a hesitation of the system which from time to time at random leaves its overall large scale relaxational behavior to describe a small loop. In the context of a dynamical evolution on an underlying torus, this transition corresponds to oscillations which surround the torus and which occasionally visit its center-hole. Figure 14(a) enlarges the region of phase space where such a switch occurs. Intersecting the trajectories with an adequate Poincaré plane yields the Poincaré map shown in Fig. 14(b). The points in the Poincaré section are not scattered in a random cloud but lie to a good approximation along a smooth curve which apparently is not a closed curve since the dynamics does not cover ergodically the surface of the torus. The associated circle map is illustrated in Fig. 14(c); it strongly suggests that the dynamics is described by the iteration of a deterministic law. A careful examination of the slope of the so-reconstructed 1D map as evaluated at the unstable fixed point (relaxation oscillations) discards de-

finitively type-I intermittency. From the negative value of the slope, one suspects a period-doubling bifurcation (slope $= -1$) rather than a saddle-node bifurcation (slope $= +1$). However, within our experimental resolution in the flow rate, we are not able to decide whether the period-doubling bifurcation is subcritical (type-III intermittency[22]) or supercritical (classical cascade of period-doubling bifurcations[65–67]); for a more detailed discussion see Ref. 68.

2. Description of a chaotic state $C_3^{n,n+1}$: $\lambda \sim 0.55$ ml/min

When we increase the flow rate beyond the transition value, we first observe a decrease in the number of large amplitude oscillations in a basic pattern, while the number of small amplitude oscillations remains unchanged, i.e., equal to one. Then, from $\lambda = 0.4$ to 0.55 ml/min, the number of large amplitude oscillations is locked to 3, and we go through periodic and chaotic states with patterns which contain more and more small amplitude oscillations. As seen in Figs. 13(d) and 13(e) for $C_3^{1,2}$ and $C_3^{4,5}$, respectively, the chaotic states are easily distinguishable from their characteristic broadband power spectra. Let us focus on $C_3^{4,5}$ (Fig. 15). The chaotic aspect of the corresponding signal is contained in the small amplitude oscillations: their number is distributed at random between 4 and 5 while their amplitudes vary from one pattern to the next one [as clearly seen on the last small amplitude oscillation in Figs. 13(e) and 15(a)]. On the other hand, when focusing on the small amplitude oscillations, two stages can be distinguished on the phase portraits in Figs. 13(e) and 15(b): a spiralling in behavior followed by a spiralling out which looks very much like an intrusion of the trajectories in the center hole of a torus. The sensitive dependence on initial conditions seems to be located in the neighborhood of the two underlying saddle foci (see paper II), while the large amplitude oscillations only ensure a nonlinear reinjection mechanism. Both ingredients to generate chaos[33,34] are present and thus it is not surprising that the whole set of points of the corresponding Poincaré map [Fig. 15(c)] do not spread throughout the plane, but always fall in one of the "islands" which resemble segments of a closed curve.

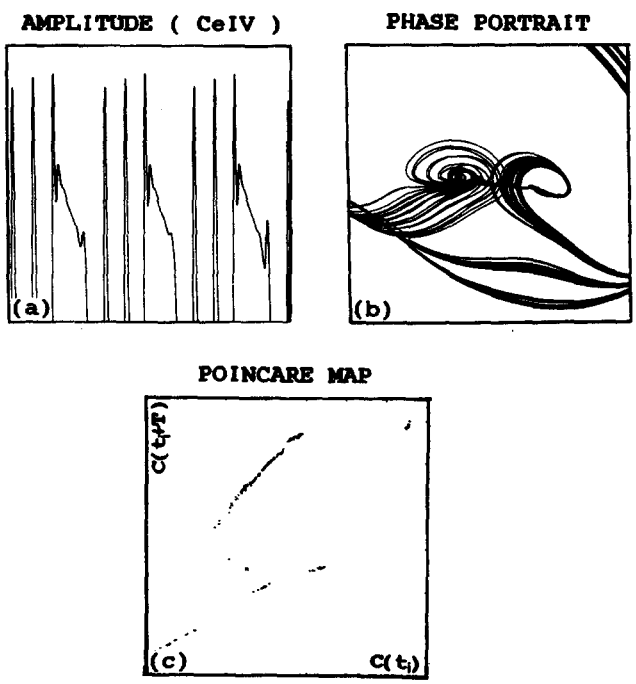

FIG. 15. A chaotic state which belongs to the periodic–chaotic sequence reported in Fig. 13; $\lambda = 0.55$ ml/min: $C_3^{4,5}$. (a) An enlargement of the time series; (b) an enlargement of the phase portrait shown in Fig. 13(e) which accounts for the spiralling in and spiralling out behavior of the trajectory; (c) a Poincaré map.

At this point let us emphasize that as enlightened by the reconstruction of the phase portraits, the chaos in this experiment is rather thin and located in a small region of the phase space where two saddle foci exist. This is quite different from the chaos observed in the Texas experiment[15,17–19] which spreads out in a broad region of phase space where (at least as far as the first steps of the periodic–chaotic sequence are concerned) only one saddle focus manifests itself without any evidence of toroidal motion.

3. Farey tree ordering and hysteresis phenomenon

When increasing further the flow rate, the system abruptly jumps from $C_3^{4,5}$ to P_2^1 for $\lambda = 0.55$ ml/min. Then, as before, while the number of large amplitude oscillations remains equal to 2, the number of small amplitude oscillations in a "motif"[69] keeps increasing and we observe successively P_2^1, P_2^2, P_2^3 which are periodic states with winding number $W = 1/3, 1/4, 1/5$, respectively. Now if we look more carefully at the parameter range [0.55 ml/min, 0.60 ml/min], we can stabilize the system for $\lambda = 0.57$ ml/min into the periodic state $P_2^{1,2}$, whose motif is $L^2S^1L^2S^2$, where L and S stand for large and small amplitude oscillations, respectively. This periodic state has the winding number $W = 2/7 = (1+1)/(3+4)$, and according to the Farey tree relationship,[63] it lies in between periodic states with winding numbers 1/3 and 1/4, i.e., P_2^1 and P_2^2. Moreover as predicted by the theory, $P_2^{1,2}$ exists on a range which is experimentally much smaller than the corresponding ranges for the bordering states P_2^1 and P_2^2. We are convinced that with a more systematic investigation of intermediate flow rate values which would require a better experimental resolution, we could, like in the Maselko and Swinney's experiment,[61,62] detect more periodic states satisfying the Farey tree ordering.

Unlike this last experiment, however, we do observe different attractors concurrently which comes with a hysteresis phenomenon. For example, when increasing the flow rate from $\lambda = 0.4$ to 0.55 ml/min, the system goes through the sequence $P_3^1, C_3^{1,2}, P_3^2, P_3^3, C_3^{4,5}, P_2^1$. Now if we reverse the variation of the flow rate and decrease λ from 0.55 to 0.4 ml/min, on this whole parameter range the system remains in the periodic state P_2^1 before switching directly to P_3^1, squeezing all the previously observed intermediate states. This suggests the coexistence of P_2^1 with this set of intermediate states, phenomenon which is to be directly associated with the existence of deterministic chaos as explained in paper II.

4. The last steps of the periodic-chaotic sequence

When λ reaches a value of about 0.72 ml/min, the dynamics is chaotic of the form C_1^n with only one large oscilla-

tion in a motif together with a lot of small amplitude oscillations. As seen on the phase portrait in Fig. 13(h), the sequence seems to end in a heteroclinic orbit[34] which connects the two saddle foci (see paper II). Indeed, although we are not too far from such a structurally unstable situation, the striking slowing down of the dynamics anticipate the appearance of a stable steady state. This transition is actually observed for $\lambda = 0.73$ ml/min. Within our experimental resolution, we cannot assert whether or not there is any hysteresis effect. To conclude, let us mention that all along this one parameter experimental path there has been no evidence for the existence of quasiperiodic states.

B. About the effects of the reagent concentrations and the temperature on the periodic–chaotic sequences

We have also constrained the BZ reaction with slightly different sets of parameters; with a change in the reagent concentrations or a temperature variation, we have observed very similar periodic–chaotic sequences. In particular, the main trends of these sequences are unaffected: when increasing the flow rate the number of large amplitude oscillations in a motif has a tendency to decrease while for a given number of large amplitude oscillations, the number of small amplitude oscillations keeps growing. According to the conditions we conduct the experiment, however, one can observe after the transition from the original relaxation oscillations, periodic as well as chaotic states which present motifs involving more or less large amplitude oscillations. In particular, in the experiment described at the beginning of this section (Experiment 4) which corresponds to a change in the reagent concentrations and from which we have extracted the chaotic state $C^4_{7,8,9}$ described in Fig. 12, the first periodic states immediately following the transition to chaos contain about ten large amplitude oscillations per motif, that is much more than in the periodic chaotic sequence described in Fig. 13. Again, the ultimate chaotic states C^n_m which precede the transition to the flux branch, may retain much more than one large amplitude oscillation in a motif: in the experiment corresponding to Fig. 12, the sequence ends with the chaotic state C^n_5. Quite the same features have been observed when moving down the temperature from 43 to 25 °C in the experiment described in Sec. IV A.

At this point, one must mention that with a different set of constraints the spiralling in effect is not apparent either on the time series or in the phase portrait. This suggests that the first focus does not affect the dynamics anymore. In this case, any reference to an evolution on an underlying (fractal) torus becomes quite questionable. We reach therefore situations out of the scope of the present paper since the dynamics has lost any memory of the original quasiperiodic regime.

C. About the effect of the stirring rate on the periodic–chaotic sequences

The effect of the stirring rate on nonlinear kinetics has been recently emphasized[70–74] and one may wonder about its correlation with actual nonperiodic regimes. We have performed several experiments on the BZ system which differ only by the value of the stirring rate in the reactor. Figure 16 illustrates two of these experiments which have been conducted up to a certain value of the flow rate, in the same experimental conditions as in Experiment 5. In the first one, we increase λ up to $\lambda = 0.55$ ml/min, and let the transients relax in order to position the system in the periodic state P^1_2; then we raise the stirring rate from 600 to 1000 rpm and we observe a transition to a nonperiodic state $C^{1,2}_2$ [Fig. 16(a)]. Such an experiment may cast a doubt on the deterministic interpretation of the observed nonperiodic states if we associate stirring rate with noise. However, if such states are nothing other than noise induced states, how can we understand the noise induced order transition observed in the experiment illustrated in Fig. 16(b) where an increase in the stirring rate initiates a transition[75,76] from the chaotic state $C^{1,2}_3$ to the periodic state P^3_5? This last experiment is thus rather intriguing in the context of a stochastic interpretation.

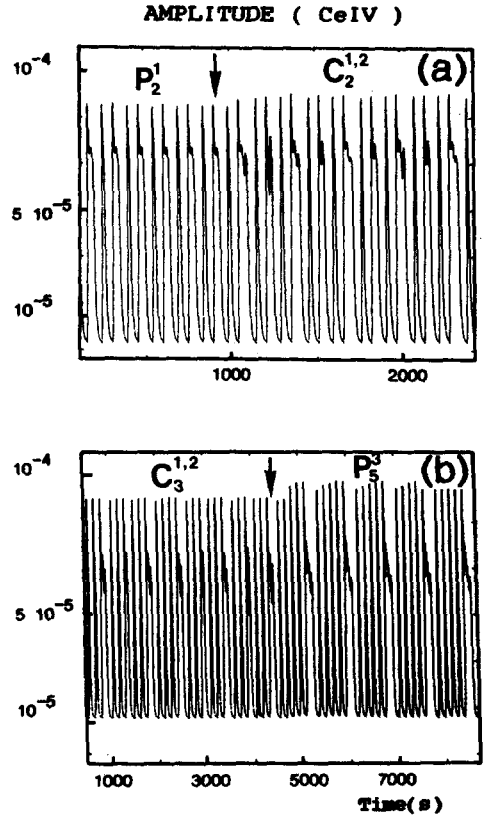

FIG. 16. The arrows indicate a switch in the stirring rate from 600 to 1000 rpm. The experimental conditions are the same as in Fig. 13. (a) $\lambda = 0.55$ ml/min: system tips from P^1_2 to $C^{1,2}_2$; (b) $\lambda = 0.45$ ml/min: the system displays a "noise induced order transition" from $C^{1,2}_3$ to P^3_5.

Actually we did perform a few experimental investigations of the periodic–chaotic sequence described in Sec. IV A with a different value of the stirring rate (1000 instead of 600 rmp) in the reactor. The main outcome of this study is that the stirring rate is a parameter which seems to play the same role as the reagent concentrations and the bath temperature. The overall effect of a change in the stirring rate is simply a deformation of the periodic–chaotic sequence with respect to the control parameter, i.e, the flow rate.

V. CONCLUSION

Recent progress in the analysis of the experimental behaviors of the BZ reaction was made possible by the development of a new tool for data analysis: the reconstruction of phase-space trajectories from a single time series. Then, from Poincaré maps and 1D maps which have been deduced from these phase portraits, several well-known routes leading to chaos have been unambiguously recognized, i.e., period doublings and intermittency. Our contribution here enlarges the already rich variety of dynamical behavior experimentally detected in the BZ reaction through the discovery of quasiperiodicity. The domain of existence in parameter space of these doubly periodic regimes is rather limited and with a slight change in the constraints we have observed a transition to chaos which comes with the breaking of the underlying torus into a fractal object.

Nevertheless, the most persuasive feature of the BZ reaction remains the sequences of periodic–chaotic states formed from combinations of large and small amplitude oscillations. These sequences have been extensively studied, experimentally as well as numerically, and shown to exist in a wide range of parameters. For a long time the status of the nonperiodic states has been at the heart of controversial arguments. Our approach to these sequences illustrates a dynamical evolution involving two characteristic frequencies. The existence of an underlying torus is however rather obscured by the strong relaxation-type character of the large amplitude oscillations. In addition, the sensitive dependence on initial conditions manifests itself essentially through the small amplitude oscillations, while the relaxation oscillations only ensure a nonlinear reinjection mechanism. Thus the chaos is located in a tiny region of phase space which does not make easy any experimental investigation. We succeed to identify several chaotic states at different stages of these sequences. It is true that these chaotic states are very sensitive to unavoidable noise arising from fluctuations in the control parameters; but *noise only affects the observation of these states* (it can even mask chaos) *and not their origin which is deterministic and results from the nonlinear complexity of the BZ kinetics*. Such an experimental outcome will be strengthened in the following paper II where numerical simulations of a seven variable Oregonator model together with a theoretical analysis based on dynamical systems and bifurcation theories will allow us to conclude definitively that deterministic chaos exists in these sequences and to discard once and for all any kind of stochastic objections. We refer the reader to Argoul's thesis,[77] which collects most of our experimental investigations of the alternating periodic–chaotic sequences in the BZ reaction.

ACKNOWLEDGMENTS

We are very grateful to H. L. Swinney for stimulating discussions and to N. Kreisberg for a careful reading of the manuscript. This research has been supported by a CNRS Grant (ATP "Mathématiques appliquées et méthodes numériques performantes").

[1] B. P. Belousov, Sb. Ref. Radiat. Med. (Collection of Abstracts on Radiation Medicine, Medzig, Moscow 1958), p. 145.
[2] A. M. Zhabotinskii, Biophysics **9**, 329 (1964).
[3] K. R. Graziani, J. L. Hudson, and R. A. Schmitz, Chem. Eng. J. **12**, 9 (1976).
[4] R. A. Schmitz, K. R. Graziani, and J. L. Hudson, J. Chem. Phys. **67**, 3040 (1977).
[5] O. E. Rossler and K. Wegmann, Nature **271**, 89 (1978).
[6] K. Wegmann and O. E. Rossler, Z. Naturforsch. Teil A **33**, 1179 (1978).
[7] J. L. Hudson, M. Hart, and D. Marinko, J. Chem. Phys. **71**, 1601 (1979).
[8] C. Vidal, J. C. Roux, A. Rossi, and S. Bachelart, C. R. Acad. Sci. (Paris) Ser. C **289**, 73 (1979).
[9] P. G. Sorenson, Ann. N. Y. Acad. Sci. **316**, 667 (1979).
[10] H. Nagashima, J. Phys. Soc. Jpn. **49**, 2427 (1980).
[11] C. Vidal, J. C. Roux, S. Bachelart, and A. Rossi, Ann. N. Y. Acad. Sci. **357**, 377 (1980).
[12] D. Ruelle, Trans. N. Y. Acad. Sci. **35**, 66 (1973).
[13] J. C. Roux, A. Rossi, S. Bachelart, and C. Vidal, Phys. Lett. A **77**, 391 (1980).
[14] J. L. Hudson and J. C. Mankin, J. Chem. Phys. **74**, 6171 (1981).
[15] J. C. Roux, J. S. Turner, W. D. McCormick, and H. L. Swinney, in *Nonlinear Problems: Present and Future*, edited by A. R. Bishop, D. K. Campbell, and B. Nicolaenko (North-Holland, Amsterdam, 1982), p. 409.
[16] P. Collet and J. P. Eckmann, *Iterated Maps of the Interval as Dynamical Systems* (Birkhauser, Boston, 1980).
[17] J. C. Roux and H. L. Swinney, in Ref. 41, p. 33.
[18] R. H. Simoyi, A. Wolf, and H. L. Swinney, Phys. Rev. Lett. **49**, 245 (1982).
[19] J. C. Roux, R. H. Simoyi, and H. L. Swinney, Physica D **8**, 257 (1983).
[20] A. Wolf, J. B. Swift, H. L. Swinney, and J. A. Vastano, Physica D **16**, 285 (1985).
[21] Y. Pomeau, J. C. Roux, A. Rossi, S. Bachelart, and C. Vidal, J. Phys. Lett. **42**, L271 (1981).
[22] P. Manneville and Y. Pomeau, Phys. Lett. A **75**, 1 (1979); Commun. Math. Phys. **74**, 189 (1980).
[23] N. Ganapathisubramanian and R. M. Noyes, J. Chem. Phys. **76**, 1770 (1982).
[24] R. M. Noyes, in *Stochastic Phenomena and Chaotic Behavior in Complex Systems*, edited by P. Schuster (Springer, Berlin, 1984), p. 107.
[25] P. Gray and S. K. Scott, J. Phys. Chem. **89**, 22 (1985).
[26] R. J. Fields, E. Koros, and R. M. Noyes, J. Am. Chem. Soc. **94**, 8649 (1972).
[27] D. Edelson, R. J. Field, and R. M. Noyes, Int. J. Chem. Kinet. **7**, 417 (1975).
[28] R. J. Fields and R. M. Noyes, J. Chem. Phys. **60**, 1877 (1974).
[29] R. J. Fields, J. Chem. Phys. **63**, 2284 (1975).
[30] K. Showalter, R. M. Noyes, and K. Bar-Eli, J. Chem. Phys. **69**, 2514 (1978).
[31] I. B. Schwartz, Phys. Lett. A **102**, 25 (1984).
[32] J. Rinzel and I. B. Schwartz, J. Chem. Phys. **80**, 5610 (1984).
[33] V. I. Arnold, *Supplementary Chapters to the Theory of Differential Equations* (Nauka, Moscow, 1978).
[34] J. Guckenheimer and P. Holmes, *Nonlinear Oscillations, Dynamical Systems and Bifurcations of Vector Fields* (Springer, Berlin, 1984).
[35] F. Takens, *Lecture Notes in Maths 898*, edited by D. A. Rand and L. S. Young (Springer, Berlin, 1981), p. 366.
[36] H. Froehling, J. P. Crutchfield, J. D. Farmer, N. H. Packard, and R. S. Shaw, Physica D **3**, 605 (1981).
[37] J. E. Marsden and M. McCraken, *Hopf Bifurcation and its Applications*, Appl. Math Sci. 19 (Springer, New York, 1976).
[38] G. Iooss and D. D. Joseph, *Elementary Stability and Bifurcation Theory* (Springer, New York, 1980).
[39] G. Iooss, *Bifurcation of Maps and Applications* (North-Holland, Amsterdam, 1979).
[40] P. Richetti, J. C. Roux, F. Argoul, and A. Arneodo, J. Chem. Phys. **86**, xxxx (1987).
[41] *Nonlinear Phenomena in Chemical Dynamics*, edited by C. Vidal and A. Pacault (Springer, Berlin, 1981).
[42] *Nonequilibrium Dynamics in Chemical Systems*, edited by C. Vidal and A. Pacault (Springer, Berlin, 1984).
[43] *Temporal Order*, edited by N. I. Jaeger, G. Schultz-Ekloff, and P. J. Plath, (Springer, Berlin, 1984).
[44] J. P. Eckmann, Rev. Mod. Phys. **53**, 643 (1981), and references therein.
[45] E. Ott, Rev. Mod. Phys. **53**, 655 (1981), and references therein.
[46] W. F. Langford, in *Nonlinear Dynamics and Turbulence*, edited by G.

Iooss and D. D. Joseph (Pitman, New York, 1982).
[47]J. C. Roux, P. Richetti, A. Arneodo, and F. Argoul, J. Mec. Th. Appl. (Numero special) 77 (1984).
[48]P. De Kepper, Thesis, Bordeaux, 1978.
[49]J. Boissonade, Thesis, Bordeaux, 1980.
[50]F. Argoul (to be published).
[51]P. De Kepper and J. Boissonade, J. Chem. Phys. **75**, 189 (1981).
[52]F. Argoul and J. C. Roux, Phys. Lett. A **108**, 426 (1985).
[53]J. H. Curry and J. A. Yorke, Lect. Notes Math. **668**, 48 (1978).
[54]D. G. Aronson, M. A. Chory, G. R. Hall, and R. P. McGehee, Commun. Math. Phys. **83**, 303 (1982).
[55]M. Dubois, P. Berge, and V. Croquette, J. Phys. Lett. **43**, L295 (1982).
[56]J. C. Roux and A. Rossi, in Ref. 42, p. 141.
[57]J. C. Roux, in *Singularities and Dynamical Systems*, edited by S. N. Pnevmatikos (Elsevier, New York, 1985), p. 345.
[58]S. Bachelart, Thesis, Bordeaux, 1981.
[59]C. Vidal, S. Bachelart, and A. Rossi, J. Phys. (Paris) **43**, 7 (1982).
[60]J. C. Roux, Physica D **7**, 57 (1983).
[61]J. Maselko and H. L. Swinney, Phys. Scr. **52**, 269 (1984).
[62]H. L. Swinney and J. Maselko, Phys. Rev. Lett. **55**, 2366 (1985), and unpublished results.
[63]G. H. Hardy and E. M. Wright, *An Introduction of the Theory of Numbers* (Clarendom, Oxford, 1965).
[64]D. Ruelle, Math. Intelligencia **2**, 126 (1980).
[65]S. Grossman and S. Thomae, Z. Naturforsch. Teil A **32**, 1353 (1977).
[66]M. J. Feigenbaum, J. Stat. Phys. **19**, 25 (1978); **21**, 669 (1979).
[67]P. Coullet and C. Tresser, J. Phys. (Paris), Colloq. **39**, C5-25 (1978); C. Tresser and P. Coullet, C. R. Acad. Sci. (Paris) **287**, 577 (1978).
[68]A. Arneodo, P. Richetti, N. Kreisberg, W. McCormick, and H. L. Swinney (in preparation).
[69]C. Lobry and R. Lozy, in Ref. 41, p. 67.
[70]J. C. Roux, P. De Kepper, and J. Boissonade, Phys. Lett. A **97**, 168 (1983).
[71]J. Boissonade, J. C. Roux, H. Saadaoui, and P. De Kepper, in Ref. 42, p. 172.
[72]W. Horsthemke and L. Hannon, J. Chem. Phys. **81**, 10 (1984).
[73]G. Dewel, P. Borckmans, and D. Walgraef, Phys. Rev. A **31**, 3 (1985).
[74]G. Nicolis and H. Frisch, Phys. Rev. A **31**, 439 (1985).
[75]K. Matsumoto and I. Tsuda, J. Stat. Phys. **31**, 87 (1983).
[76]K. Matsumoto, J. Stat. Phys. **34**, 111 (1984).
[77]F. Argoul, Thesis, Bordeaux, 1985.